FEMS Microbes, 2024, 5, xtae030
DOI: 10.1093/femsmc/xtae030
Advance access publication date: 25 September 2024
Research Article – Microbes & Metabolism

Arginine impacts aggregation, biofilm formation, and antibiotic susceptibility in *Enterococcus faecalis*

Alex P. Snell[1], Dawn A. Manias[1], Reham R. Elbehery[1,2], Gary M. Dunny[1], Julia L.E. Willett[1,*]

[1]University of Minnesota Medical School, Minneapolis, MN 55455, United States
[2]Present address: Drug Radiation Research Department, Egyptian Atomic Energy Authority, Cairo 11787, Egypt
*Corresponding author. Department of Microbiology and Immunology, University of Minnesota Medical School, Minneapolis 55455, United States.
E-mail: jwillett@umn.edu
Editor: [Kathleen Scott]

Abstract

Enterococcus faecalis is a commensal bacterium in the gastrointestinal (GI) tract of humans and other organisms. *E. faecalis* also causes infections in root canals, wounds, the urinary tract, and on heart valves. *E. faecalis* metabolizes arginine through the arginine deiminase pathway, which converts arginine to ornithine and releases ATP, ammonia, and CO_2. *E. faecalis* arginine metabolism also affects virulence of other pathogens during co-culture. *E. faecalis* may encounter elevated levels of arginine in the GI tract or the oral cavity, where arginine is used as a dental therapeutic. Little is known about how *E. faecalis* responds to growth in arginine in the absence of other bacteria. To address this, we used RNAseq and additional assays to measure growth, gene expression, and biofilm formation in *E. faecalis* OG1RF grown in arginine. We demonstrate that arginine decreases *E. faecalis* biofilm production and causes widespread differential expression of genes related to metabolism, quorum sensing, and polysaccharide synthesis. Growth in arginine also increases aggregation of *E. faecalis* and promotes decreased susceptibility to the antibiotics ampicillin and ceftriaxone. This work provides a platform for understanding how the presence of arginine in biological niches affects *E. faecalis* physiology and virulence of surrounding microbes.

Keywords: *Enterococcus faecalis*; biofilms; arginine deiminase; arginine metabolism; antibiotic resistance

Introduction

Enterococcus faecalis is found as a low-abundance commensal bacterium in the gastrointestinal (GI) tract of humans, animals, and insects (Gilmore et al. 2013, Lebreton et al. 2017). *E. faecalis* can be highly resistant to antibiotics and other antimicrobial treatments, and it forms robust biofilms on surfaces (Gilmore et al. 2020, Tan et al. 2020). Outside of the GI tract, *E. faecalis* is a prevalent cause of opportunistic infections in wounds, heart valves, implanted devices, the urinary tract, and root canals (Goh et al. 2017, García-Solache and Rice 2019, Tan et al. 2020). In these environments, *E. faecalis* interacts with other microbes and promotes virulence of pathogens, including *Clostridioides difficile*, uropathogenic and enterohemorrhagic *Escherichia coli*, *Pseudomonas aeruginosa*, *Proteus mirabilis*, and *Staphylococcus aureus* (Keogh et al. 2016, Tien et al. 2017, Gaston et al. 2020, 2021, Ch'ng et al. 2022, Smith et al. 2022, Tan et al. 2022). A key nutrient mediating many of these interactions is arginine. *E. faecalis*, like many bacteria, can metabolize L-arginine as an energy source through the arginine deiminase (ADI) pathway, producing ATP, L-ornithine, CO_2, and NH_3 as byproducts (Deibel 1964, Barcelona-Andrés et al. 2002). Export of L-ornithine by *E. faecalis* promotes siderophore synthesis and biofilm production by *E. coli*, and breakdown of arginine by *E. faecalis* promotes virulence of *C. difficile* (Keogh et al. 2016, Smith et al. 2022). Disrupting the ADI pathway can also affect *E. faecalis* biofilm formation *in vitro* (Manias and Dunny 2018, Willett et al. 2019).

The ADI pathway is relevant to health and disease in the oral cavity (Nascimento 2018). Production of NH_3 by the oral microbiome and the resulting increase in pH can protect against acidification caused by bacteria such as *Streptococcus mutans*, as low pH can lead to the development of caries (cavities) (Burne and Marquis 2000). L-arginine reduces biofilm formation independent of growth inhibition in a multi-species biofilm with oral bacteria and leads to growth suppression of caries-causing *S. mutans* in biofilms with *Streptococcus gordonii* and *Actinomyces naeslundii* (Kolderman et al. 2015, He et al. 2016). Application of exogenous arginine results in destabilization and disruption of pre-formed biofilms grown from *S. gordonii* monocultures or a mixed oral bacterial community (Kolderman et al. 2015, Gloag et al. 2021). In patients with caries, the use of toothpaste supplemented with arginine led to an increase in ADI pathway activity and an increase in plaque species that are associated with health instead of disease (Nascimento et al. 2014). Outside of the oral cavity, the ADI pathway also affects biofilms, antibiotic tolerance, gene expression, and pathogenesis of *Streptococcus pyogenes* (Freiberg et al. 2020, Hirose et al. 2021), and exogenous arginine decreases biofilm formation in *S. aureus* (Manna et al. 2022). Despite the importance of arginine catabolism and ADI pathway byproducts on biofilm formation and polymicrobial interactions involving numerous bacteria, little is known about the effect of arginine on gene expression, biofilm formation, and antimicrobial resistance in *E. faecalis*.

Our goal was to determine how arginine affects *E. faecalis* independent of polymicrobial interactions. Here, we measured changes in gene expression and biofilm formation of *E. faecalis* OG1RF after growth in arginine relative to growth in control medium without arginine. We found that, similar to other bacteria, growth in arginine decreased biofilm formation by *E. faecalis*.

Received 27 May 2024; **revised** 26 August 2024; **accepted** 24 September 2024

However, pre-formed *E. faecalis* biofilms were not susceptible to destabilization by high concentrations of arginine as has been reported for oral streptococci. We also found widespread changes in gene expression in arginine-grown cells relative to control cells, including changes in expression of metabolic pathways and virulence factors. Growth in arginine promoted aggregation, increased cell envelope permeability, and increased resistance to select cell wall-targeting antibiotics, including ampicillin. Together, this demonstrates that the presence of arginine induces global changes in the growth and physiology of *E. faecalis*, which will serve as the basis for future studies on how these changes affect monomicrobial and polymicrobial infections involving *E. faecalis*.

Materials and methods

Bacterial strains, growth conditions, and reagents

All strains used are listed in Table S3. Bacterial stocks were maintained at −80°C in 25% glycerol (w/v). Strains were routinely grown in complex basal medium (CBM; Deibel 1964) or brain–heart infusion broth (BHI, Difco). Media was supplemented with 1% agar for solid plates. Unless otherwise noted, strains were cultured under static conditions. Where indicated, cultures were supplemented with arginine, glucose, and glycine (Sigma) from 1 M stock solutions that were prepared in water and filter sterilized. Antibiotic discs (BD BBL) were purchased from Fisher Scientific.

RNA sequencing and analysis

OG1RF was diluted to OD600 = 0.02 and grown in CBM with or without 25 mM arginine for 6 h. Two independent biological replicates were used for each condition. Planktonic cells (~2×10^9 CFU) were mixed with a 2:1 volume of RNAprotect (Qiagen), pelleted, and stored at −80°C. Biofilms were grown on Aclar coupons, which were rinsed in phosphate-buffered saline with 10 mM potassium at pH 7.4 and scraped with a razorblade to remove cells. Cells were pelleted and stored at −80°C. Pellets were resuspended in 200 µl TE buffer (10 mM Tris pH 8.0 and 1 mM ethylenediaminetetraacetic acid (EDTA)) supplemented with 30 mg/ml lysozyme and 500 U/ml mutanolysin and incubated at 37°C for 10 min, after which RNA was extracted using a Qiagen RNeasy kit following the manufacturer's instructions. Lysozyme and mutanolysin were purchased from Sigma. Residual genomic DNA was removed using Turbo DNase (Ambion) following the manufacturer's protocol for two DNase treatments (rigorous method). Complete removal of DNA was confirmed using polymerase chain reaction (PCR) with oligos JD460s and JD461as (Table S3). rRNA was depleted using MICROBExpress (Ambion). RNA was sent to the University of Minnesota Genomics Center for TruSeq stranded library preparation and sequencing on a single lane of an Illumina NextSeq 550 in mid-output mode (75-bp paired-end reads). Sequencing quality was evaluated using FastQC (Andrews 2010). Reads were trimmed with Trimmomatic (Bolger et al. 2014) and imported into Rockhopper for analysis using standard settings (McClure et al. 2013, Tjaden 2015). Reads were aligned against a custom OG1RF reference genome in which intergenic regions are annotated. Fold changes (log2FC) were calculated from Rockhopper expression values, and q-values ≤ 0.05 were considered statistically significant.

Growth measurements

For growth curves, OG1RF cultures were grown overnight in 3 ml of CBM. Cells were diluted 1:100 in a 96-well plate (Corning 3595) using untreated CBM or CBM supplemented with arginine (25 or 50 mM), glucose (25 mM), glycine (25 or 50 mM), or a vehicle control for a final volume of 200 µl. Three independent biological replicates (each with three technical replicates) were performed. Plates were sealed (Microseal B plate seals, Bio-Rad) and incubated in a Biotek Epoch 2 microplate reader without shaking at 37°C for 15 h. The A_{600} was measured every 30 min. Technical replicates were averaged, and the average of all biological replicates was plotted. For quantification of colony forming units, OG1RF cultures were grown in glass culture tubes in 3 ml CBM supplemented with arginine, glycine, and glucose (at 25 and 50 mM). After 24 h, cultures were diluted (10-fold serial dilutions) and spotted onto agar plates. CFU/ml was quantified after 24 h incubation.

Biofilm assays

Cultures were grown overnight at 37°C in 3 ml of CBM. Cells were diluted 1:50 in a 96-well plate (Corning 3595) in 200 µl of CBM supplemented with arginine or glycine (25 or 50 mM). Three independent biological replicates were done for each condition. Plates were incubated in a humidified plastic container at 37°C for 6 or 24 h. Growth of the cells was quantified by measuring the A_{600} using a Biotek Epoch 2 microplate reader. The planktonic cells and media were removed by washing three times with de-ionized water. After drying, the plates were then stained with 0.1% w/v safranin (Sigma) for 20 min, at which point the plates were washed again with de-ionized water. For post-growth treatment of biofilms with arginine, glycine, or glucose, biofilms were grown as described above, and A_{600} was measured. A volume of 100 µl of the indicated compound was added to each well for 20 min, after which biofilms were washed, dried, and stained with safranin. Stained biofilm material was quantified by measuring A_{450}. The biofilm index was then calculated as A_{450}/A_{600} as a representation of biofilm biomass relative to planktonic cell growth.

Fluorescence microscopy of biofilms

OG1RF cultures were grown overnight in 3 ml of CBM at 37°C and diluted 1:50 into an optically clear 96-well plate (Nunc MicroWell tissue culture-treated optical bottom plates). Each well contained 200 µl of CBM with or without arginine (25 and 50 mM), glucose (25 and 50 mM), or glycine (25 and 50 mM). Plates were grown in a humidified chamber at 37°C for 24 h. Plates were then washed once with phosphate buffered saline (PBS, pH 7.4), and 200 µl of formalin (10% w/v) was added at 4°C for 16 h to fix the cells. Formalin was removed with a multichannel pipette, and the plate was then washed once with PBS. A volume of 200 µl of Hoechst 33342 (Thermo Fisher Scientific) dye was added (final concentration 5 µg/ml) and incubated on the lab bench for 30 min prior to imaging. The plate was then imaged using a Keyence BZ-X810 microscope with a Chroma DAPI filter (AT350/50×) at 20× magnification. At least three images were acquired for each independent biological replicate. Images were processed using the rolling ball background subtraction feature in Fiji and cropped to 500 × 500 pixels.

Auto-aggregation assay

Strains were diluted 1:100 in 2 ml of CBM supplemented with arginine (25 or 50 mM), glycine (25 mM), or glucose (25 mM). Cultures were grown for 24 h at 37°C at which point 100 µl was removed from the top of the culture, mixed with 900 µl medium, and used to measure A_{600}. Cultures were vortexed, and another A_{600} reading was taken for the mixed culture. To quantify aggregation, the A_{600} of the unmixed culture was divided by the A_{600} culture after mixing and multiplied by 100.

Cell envelope permeability assay

OG1RF pCJK205 and *arcD*:: Tn pCJK205 were grown overnight in 3 ml of BHI with 10 µg/ml of erythromycin (Erm) at 37°C. The culture was then diluted to an A_{600} of 0.05 in 5 ml of fresh CBM (or tryptic soy broth without added dextrose), 10 µg/ml Erm, and 20 µg/ml of chlorophenol red-β-D-galactopyranoside (CPRG) supplemented with arginine (25 or 50 mM), glycine (25 mM), or glucose (25 mM). Cultures were incubated for 24 h at 37°C, at which time the A_{630} was measured. A volume of 750 µl of culture was pelleted, and the A_{570} of the supernatant was measured. To quantify CPRG cleavage relative to growth, the A_{570} value was divided by the A_{600}.

Antibiotic disc diffusion assay

CBM agar plates were supplemented with 25 mM arginine, 25 mM glucose, or left untreated. Cultures of OG1RF were grown overnight in CBM at 37°C, and 200 µl was spread onto each plate. Plates were incubated at room temperature for 15 min, after which antibiotic discs (gentamicin, ampicillin, penicillin, minocycline, vancomycin, cephalothin, ceftriaxone, and linezolid) were placed on the plate surface. Plates were then incubated for 24 h at 37°C, after which plates were imaged with a Cell Biosciences FluorChem FC3 plate reader. The zone of clearance for each antibiotic was measured in millimeters using Fiji (Schindelin et al. 2012).

Gelatinase activity assay

Overnight cultures of OG1RF were grown in 3 ml CBM at 37°C. A volume of 5 µl of the culture was spotted on CBM agar plates supplemented with 3% w/v gelatin and 25 mM arginine or glucose. Plates were incubated at 37°C for 24 h, after which they were transferred to 4°C for 24 h prior to imaging. Images were taken using a Cell Biosciences FluorChem FC3 image, and the diameter of each gelatinase halo was measured in millimeters using Fiji (Schindelin et al. 2012).

Statistical analysis

Statistical analysis was performed using GraphPad Prism (version 10.1.1). Statistical tests and the number of replicates represented by each data point are described in figure legends.

Results

Arginine promotes aggregation and decreases biofilm formation of *E. faecalis*

In *E. faecalis* and related bacteria, arginine is metabolized through the ADI pathway, which generates ATP and leads to a concomitant increase in optical density relative to unsupplemented cultures (Deibel 1964). To confirm this in our system, we used the well-studied strain OG1RF, which has been used in other studies demonstrating that arginine metabolism and ornithine production enhance virulence and polymicrobial infections (Dunny et al. 1981, Keogh et al. 2016, Smith et al. 2022). We grew OG1RF in 96-well plates using CBM supplemented with arginine (25 or 50 mM) and measured A_{600} over time. CBM was chosen as it was originally used to study arginine as an energy source in *E. faecalis* and contains potassium phosphate, sodium chloride, and yeast extract (which provides a small amount of carbon and nitrogen) (Deibel 1964). These concentrations were chosen as they have been previously used to study the ADI pathway in *E. faecalis* and biofilm formation and dispersal in oral streptococci (Deibel 1964, Barcelona-Andrés et al. 2002, Jakubovics et al. 2015). Untreated CBM or CBM supplemented with glucose (50 mM) or glycine (25 or 50 mM) was used as controls. For cultures grown with arginine, the A_{600} increased relative to untreated CBM, but the final A_{600} was not as high as glucose-grown cultures (Fig. 1A). No increase was observed with glycine. We next grew 3 ml cultures in glass tubes for 24 h and quantified CFU/ml. As expected, the CFU/ml of cultures grown with glucose was ∼0.5 log higher than untreated CBM cultures, but only a small increase (∼0.1 log) was observed with arginine supplementation (Fig. 1B). Similarly, the A_{600} of glucose-grown cultures in test tubes was higher than untreated CBM cultures, but arginine did not lead to a consistent increase in the A_{600} in these cultures as in 96-well plates (Fig. 1C). During these experiments, we observed aggregation of cells at the bottom of culture tubes and quantified the % of aggregated cells in each condition. In 50 mM arginine, the % of aggregated cells rose to ∼60% on average relative to ∼25% in untreated CBM (Fig. 1D). Aggregation also increased in glucose-grown cells to a similar level as arginine-treated cultures, but no increase was observed with glycine. Arginine-dependent aggregation was not observed in Tn mutants with insertions in the ADI pathway genes *arcABC* or *arcD*, which encode an arginine/ornithine antiporter (Fig. 1E), although these strains still aggregated when grown in glucose (Fig. S1). Together, these results suggest that catabolism of arginine by *E. faecalis* leads to an increase in aggregation.

Next, we asked how arginine affected *E. faecalis* biofilm formation, given that arginine reduces biofilm formation in other Gram-positive bacteria (Jakubovics et al. 2015, Freiberg et al. 2020, Manna et al. 2022). We grew OG1RF biofilms for 6 or 24 h in 96-well plates using the media described above and quantified safranin-stained biofilm material (A_{450}) relative to A_{600}. In early biofilms (6 h), growth in 25 and 50 mM arginine reduced OG1RF biofilm by ∼50% relative to untreated CBM, but glycine did not affect the level of biofilm produced (Fig. 2A). At 24 h, biofilm formation in arginine-supplemented cultures was reduced 60%–75% relative to untreated biofilms and those grown with glycine (Fig. 2B). We next asked whether exogenous arginine added after biofilm formation could disrupt pre-formed biofilms. Biofilms were grown for 6 or 24 h (Fig. 2C and D), after which arginine, glycine, or a buffer control was added for 20 min. No dispersal or decrease in biofilm level relative to control biofilms was observed. Surprisingly, post-growth treatment of early biofilms with glycine resulted in an increase in biofilm index values relative to control-treated biofilms, although this increase was not statistically significant. We speculate that this may be due to glycine binding to or interacting with a component of the early biofilm matrix, since this increase was not evident at 24 h. We next measured biofilm formation and destabilization in higher concentrations of arginine (100, 250, and 500 mM) that have been used therapeutically and for other studies on oral biofilms (Kolderman et al. 2015, He et al. 2016, Chakraborty and Burne 2017, Zheng et al. 2017, Nascimento 2018). We observed a 70%–95% reduction in biofilm formation when arginine was added during growth, but surprisingly, addition of 500 mM exogenous arginine did not significantly destabilize pre-formed biofilms (Fig. S2), even though this concentration was shown to disrupt oral biofilms *in vitro* (Jakubovics et al. 2015, Kolderman et al. 2015, He et al. 2016).

To test whether this disruption in biofilm formation was dependent on arginine metabolism through the ADI pathway, we cultured mutants with Tn insertions in *arcABCD* and measured biofilm formation with and without arginine. An arginine-dependent decrease in biofilm formation was not observed in the *arcABCD* Tn mutants (Fig. 2E). Interestingly, we previously ob-

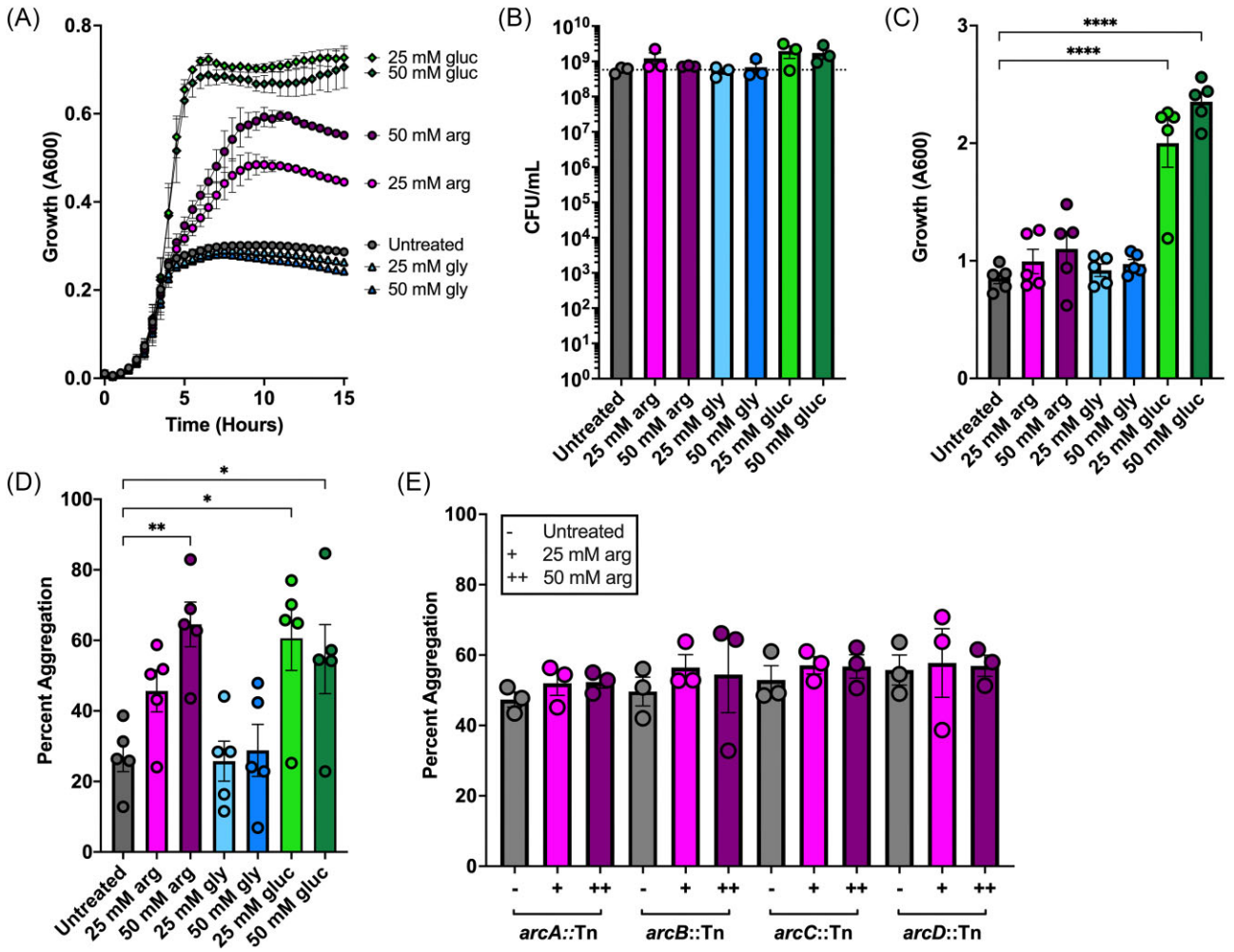

Figure 1. Growth and aggregation of *E. faecalis* OG1RF grown in arginine. (A) Microtiter plate growth curve of OG1RF grown in CBM supplemented with the indicated concentrations of arginine, glycine, or glucose. (B) CFU/ml of OG1RF grown in glass test tubes in CBM supplemented with arginine, glycine, or glucose for 24 h. (C) Absorbance at 600 nm of OG1RF grown in glass test tubes in CBM supplemented with arginine, glycine, or glucose for 24 h. (D) Aggregation assay of OG1RF grown with arginine, glycine, and glucose for 24 h. (E) Aggregation of Tn mutants with insertions in genes encoding the ADI pathway and an arginine/ornithine antiporter (*arcABCD*) after growth in untreated CBM or arginine for 24 h. In panel (A), data points represent the average of three independent biological replicates. For panels (B)–(E), each data point represents one independent biological replicate with two or three technical replicates. For all panels, error bars represent standard error of the mean. Statistical significance in panels (C) and (D) was determined by one-way ANOVA with Tukey's test for multiple comparisons. Comparisons that were not statistically significant are not shown. $^{*}P < .05$, $^{**}P < .01$, $^{***}P < .001$, $^{****}P < .0001$.

served a reduction in biofilm formation relative to parental OG1RF with these mutants in tryptic soy broth without added glucose (Willett et al. 2019), suggesting that other components of growth medium may influence biofilm formation through the ADI pathway. To ensure that this response was not specific to OG1RF, we measured microtiter plate biofilm formation after 24 h growth in the presence and absence of arginine for 10 *E. faecalis* isolates obtained from fecal samples from healthy human volunteers (Leuck et al. 2014). Arginine-dependent decreases in biofilm formation were observed for 7 of the 10 strains (Fig. 2F). Two of the strains (FVE041 and FVE071) that did not have reduced biofilm formation in the presence of arginine formed very poor biofilms in control conditions. Therefore, we conclude that arginine disruption of *E. faecalis* biofilm formation is not a strain-specific effect.

Finally, we asked how biofilm morphology was impacted by growth in arginine and used fluorescence microscopy to evaluate the appearance of biofilms grown for 24 h. OG1RF grown in unsupplemented CBM formed monolayer biofilms (Fig. 2G), similar in appearance to those observed with OG1RF (Dale et al. 2017, Korir et al. 2019, Willett et al. 2021). Biofilms grown with 25 mM arginine resembled those grown in CBM, but growth in 50 mM arginine led to the formation of biofilms with aggregates of cells. Growth in glycine resulted in monolayer biofilms similar in appearance to those grown in CBM, whereas growth in glucose resulted in biofilms with large multi-cellular aggregates, as has been previously observed in glucose-rich media (Willett et al. 2021). These data demonstrate that growth in arginine alters *E. faecalis* biofilm formation through the ADI pathway.

Transcriptional response of *E. faecalis* to arginine

Because we observed significant changes in aggregation and biofilm formation after growth in arginine, we sought to determine how arginine affects global gene expression in *E. faecalis*. We grew planktonic and biofilm cultures of OG1RF in CBM in the presence and absence of 25 mM arginine for 6 h and used RNAseq to compare differentially expressed transcripts (Table S1, Fig. 3). Relatively few loci (genes or intergenic regions) were differentially expressed in planktonic compared to biofilm

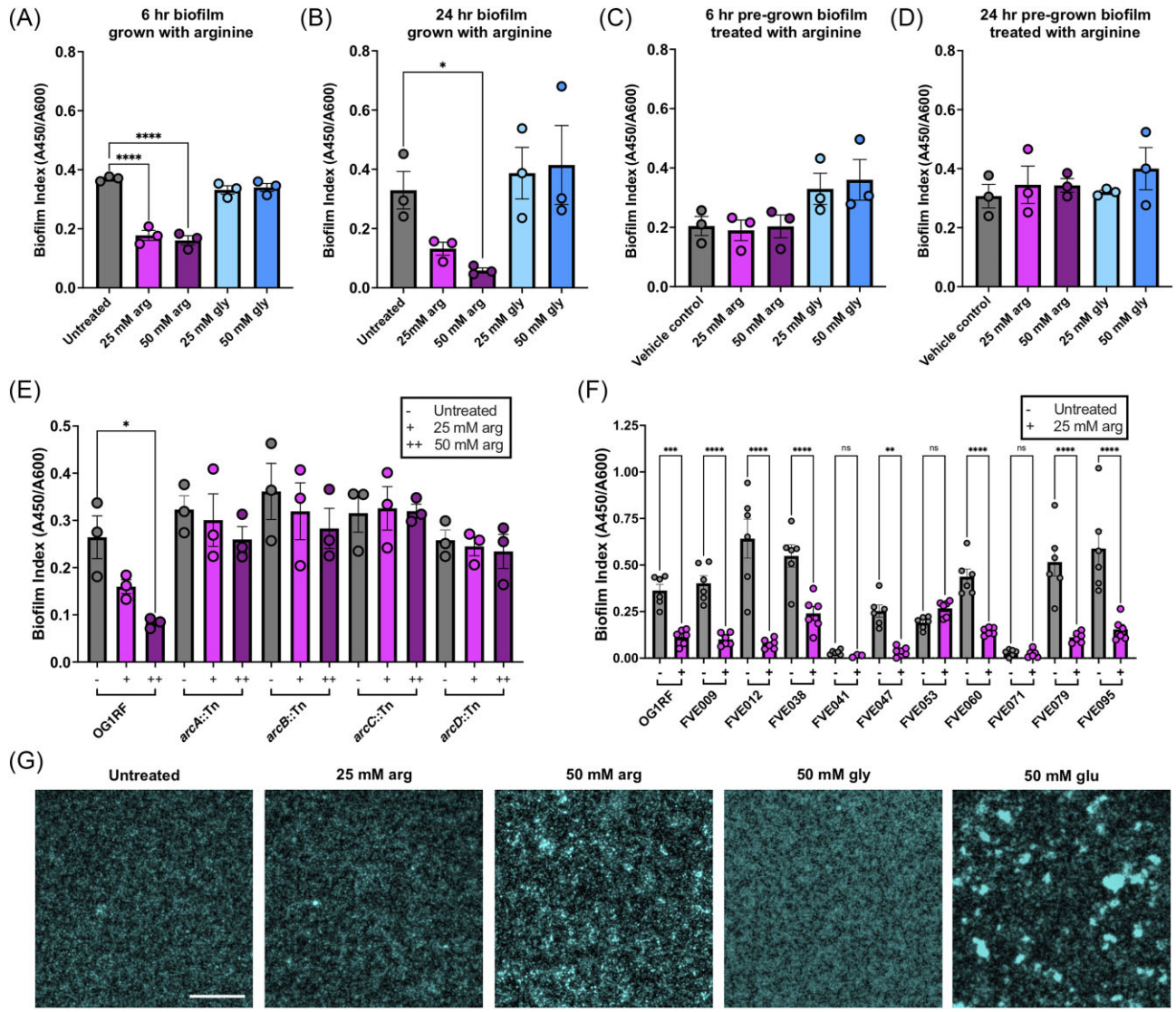

Figure 2. Arginine affects biofilm formation and structure in *E. faecalis*. Biofilm formation was measured in microtiter plates with arginine added (A) prior to growth for 6 h, (B) prior to growth for 24 h, (C) after 6 h growth, and (D) after 24 h growth. For pre-formed biofilms, arginine was added for 20 min and removed by washing. (E) 24 h microtiter plate biofilm formation of OG1RF and Tn mutants with insertions in ADI pathway genes *arcABCD*. (F) 24 h microtiter plate biofilm formation of *E. faecalis* gastrointestinal tract isolates from healthy human volunteers. (G) Fluorescence microscopy visualization of *E. faecalis* OG1RF biofilms grown for 24 h in the indicated conditions. Cells were fixed in formalin and stained with Hoechst 33342. The scale bar represents 50 µm. Images shown are representative of three independent biological replicates. For panels (A)–(F), each data point represents one independent biological replicate with three technical replicates. Error bars represent standard error of the mean. Statistical significance was determined by one-way ANOVA with Tukey's test for multiple comparisons. Comparisons that were not statistically significant are not shown. $^{*}P < .05$, $^{**}P < .01$, $^{***}P < .001$, $^{****}P < .0001$.

culture relative to the number of genes differentially expressed in the presence of arginine. A total of 34 loci were downregulated in biofilms relative to planktonic culture in the absence of arginine, and 8 were upregulated. A total of 35 loci were downregulated in biofilms relative to planktonic culture in arginine, and 8 were upregulated. In planktonic culture, 1037 loci were downregulated, and 909 were upregulated in arginine relative to no arginine. In biofilms, 922 loci were downregulated, and 963 were upregulated in arginine relative to no arginine. Of the loci upregulated in biofilms independent of arginine, most are in the *ebp* operon encoding production of pili subunits. A total of 24 loci were downregulated in biofilms relative to planktonic culture independent of arginine treatment. Of these, 21 are part of the cryptic phage02 operon spanning OG1RF_11046-11061 (McBride et al. 2007). Many of these proteins were previously identified in membrane vesicles derived from OG1RF (Afonina et al. 2021), but the role of phage02 in biofilm formation is unknown. Of the arginine-responsive loci, 842 were upregulated, and 852 were downregulated in both planktonic and biofilm cultures relative to the untreated controls. This suggests that a majority of transcriptional changes that occur during growth in arginine happen independent of growth state (biofilm or planktonic). Based on this, and because we saw significant changes in aggregation during planktonic culture, additional analysis of gene expression changes was done using the planktonic RNAseq dataset.

The 10 most highly upregulated and downregulated loci during planktonic growth in arginine are shown in Table 1. In accordance with previous work (Barcelona-Andrés et al. 2002), expression of *arcA* and *arcB* increased during growth with arginine (Table S1). The first group of highly downregulated genes, spanning

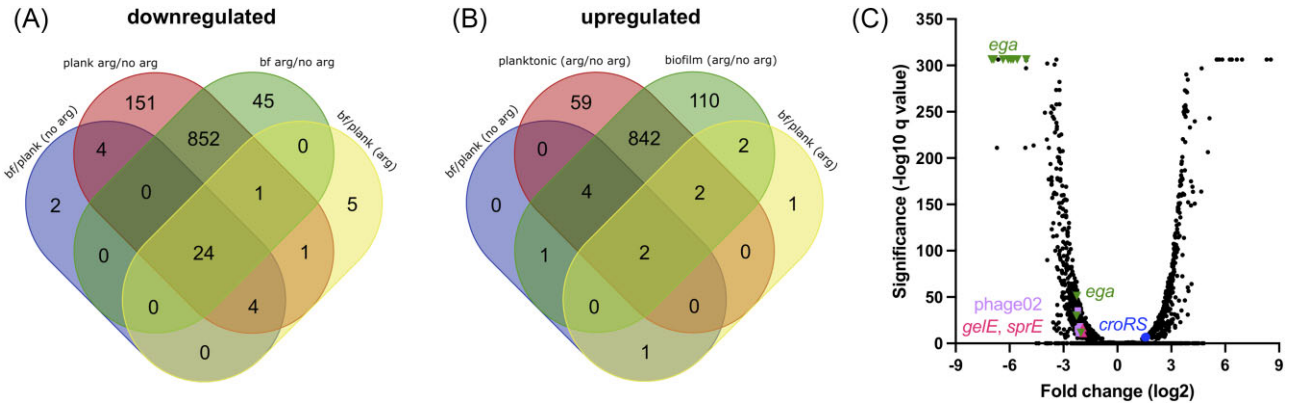

Figure 3. Differential gene expression in OG1RF after growth in arginine. Venn diagrams show (A) downregulated and (B) upregulated genes after planktonic or biofilm growth with or without arginine. (C) Volcano plot highlighting genes differentially expressed during planktonic growth in arginine relative to untreated controls. *q*-values of 0 were set to the lowest *q*-value obtained (E-306) prior to calculating $\log_{10}$ for visualization purposes.

Table 1. Genes over- and underexpressed in OG1RF after planktonic growth in arginine.

Underexpressed in arginine		
Locus tag	**Gene product**	**Log2FC**
Intergenic_988	Between OG1RF_10936 (*celA4*) and OG1RF_10937 (*celB2*)	– 6.99
OG1RF_10936 (*celA4*)	PTS system transporter subunit I	– 6.89
OG1RF_11942	Ferredoxin–NADP(+) reductase subunit alpha	– 6.70
OG1RF_10939	Hypothetical protein	– 6.64
OG1RF_10937 (*celB2*)	PTS family oligomeric beta-glucoside porter component IIC	– 6.36
Intergenic_1674	Between OG1RF_11619 and OG1RF_11620	– 6.25
Intergenic_987	In between OG1RF_10935 (*ansB*) and OG1RF_10936 (*celA4*)	– 6.07
OG1RF_10938	Hypothetical protein	– 5.93
OG1RF_11 941 (*gltA*)	Glutamate synthase	– 5.82
Intergenic_989	Between OG1RF_10937 (*celB2*) and OG1RF_10938	– 5.81
Overexpressed in arginine		
Locus tag	Gene product	Log2FC
Intergenic_446	Between OG1RF_10416 and OG1RF_10417 (*pbp2A*)	5.52
Intergenic_1362	Between OG1RF_11307 and OG1RF_11308	5.54
OG1RF_10759	Hypothetical protein	5.66
OG1RF_11308	N-acetyltransferase	5.83
OG1RF_12331	Lipase	6.25
OG1RF_11689	Hypothetical protein	6.36
OG1RF_10757 (*ppdK*)	Pyruvate phosphate dikinase	6.64
Intergenic_1750	Between OG1RF_nc10028 (*glmS*, glucosamine-6-phosphate activated ribozyme) and OG1RF_11693	6.93
OG1RF_10535	Hypothetical protein	8.30
OG1RF_10328	Peptidoglycan-binding protein	8.54

The 10 most highly over- and underrepresented transcripts (statistically significant with $q < 0.05$) are shown. Log2FC (log2 fold change) values were calculated based on growth in arginine compared to untreated conditions.

OG1RF_10935-10939, is within the recently named enteroccocal glycosylasparaginase locus (*ega*) (Combret et al. 2023). These encode an N4-(*β*-N-acetylglucosaminyl)-l-asparaginase (EgaG, OG1RF_10935), the EIIB and EIIC subunits of a lactose/cellobiose phosphotransferase system, and a pseudogene that encodes a putative oxidoreductase in other strains (Wagner et al. 1999, Combret et al. 2023). OG1RF_10933 and OG1RF_10934, which encode a GntR transcriptional regulator and a dipeptidase and are controlled by a different promoter than OG1RF_10935-10939 (Combret et al. 2023), were also downregulated, albeit to a lesser extent. The second set of highly downregulated genes includes OG1RF_11941 (encoding glutamate synthase) and OG1RF_11942 (encoding a ferredoxin-NADP+ reductase subunit), which are in an operon (OG1RF_11941-11962) that is involved in selenium and molybdenum metabolism (Zhang et al. 2008) (Table S1). These genes are not commonly found outside of *E. faecalis* and have been implicated in redox control (Gilmore et al. 2020). These gene groups suggest that *E. faecalis* may downregulate metabolic pathways involved in utilizing other nutrients such as sugars or amino acids during growth in arginine.

Unlike the downregulated genes, the genes most highly expressed during growth in arginine were not in operons or clusters in the genome (Table 1). The most overexpressed gene, OG1RF_10328, encodes a putative peptidoglycan-binding protein. OG1RF_10328 has predicted LysM and DUF4106 domains and is annotated as a peptidoglycan-binding protein (GenBank AEA93015.1). Bacterial LysM-domain proteins, such as a major *E. faecalis* autolysin involved in cell division (AtlA), typically bind N-acetylglucosamine in peptidoglycan (Béliveau et al. 1991, Eckert et al. 2006, Buist et al. 2008). OG1RF_10328 was also upregulated

in strain V583 (locus tag EF0443) after treatment with antibiotics targeting the cell envelope (Abranches et al. 2014, Darnell et al. 2019) and is part of the CroRS regulon, which responds to cell wall stress (Kellogg and Kristich 2016, Muller et al. 2018). In addition to OG1RF_10328, OG1RF_10535 and OG1RF_12331 were upregulated after exposure to antibiotics that target the cell envelope (Abranches et al. 2014) and in arginine-grown cells. OG1RF_10759 (EF1026) has similarity to a gene product involved in carbon catabolite repression in *Bacillus* (Opsata et al. 2010). Additional genes upregulated during growth in arginine include many involved in virulence and biofilm formation, including the enterococcal polysaccharide biosynthesis operon (*epa*, OG1RF_11706-11738) and *ebpABC* (OG1RF_10869-10871), which encode the Ebp pili subunits. Curiously, the quorum sensing gene *fsrA* was upregulated, but the Fsr-regulated proteinases GelE and SprE were downregulated. This suggests there may be decoupling of quorum sensing and GelE/SprE expression during growth in arginine. To validate these findings, we used an agar plate-based assay to evaluate gelatinase production of OG1RF grown on CBM agar or CBM supplemented with 25 mM arginine or 25 mM glucose. Colonies grown on plates supplemented with arginine produced gelatinase zones with smaller diameters than cells grown on unsupplemented plates or plates with glucose (Fig. S3). This reduced GelE activity supports the changes in *gelE* gene expression observed using RNAseq.

Comparison of *E. faecalis* growth in arginine and alkaline stress

Ammonia generation as a byproduct of the ADI pathway during growth in arginine could put cells under alkaline stress, and previous work found that growth of *E. faecalis* at pH 10 resulted in biofilms with less surface coverage relative to unadjusted medium (Barcelona-Andrés et al. 2002, Ran et al. 2015). We measured the pH of our *E. faecalis* cultures grown in untreated CBM or medium supplemented with arginine, glycine, and glucose. The pH of cultures grown in 25 or 50 mM arginine increased from pH 7 to approximately pH 8 after 6 h and pH 9 after 24 h (Fig. S4). Although *E. faecalis* is highly tolerant to pH stress (Gaca and Lemos 2019), we were curious whether any differential gene expression in our RNAseq could be attributed to increased pH. To determine this, we compared our data to previously published studies on gene expression and adaptation to growth at high pH. First, we examined a study of the transcriptional response of *E. faecalis* ATCC 33186 to growth at pH 10 (Ran et al. 2015). Of the 613 genes differentially expressed at pH 10, we identified 253 as also differentially regulated in our arginine RNAseq (Table S2). However, only 33 genes had the same pattern of gene expression (up or downregulated in both studies). The 17 commonly upregulated genes included 7 encoding hypothetical proteins and 4 encoding ribosomal proteins. The 16 commonly downregulated genes included those involved in pyrimidine metabolism (OG1RF_11425-11429) and a putative iron-siderophore ABC transporter (OG1RF_12351-12354). Next, we compared our results to studies showing that growth at high pH increased expression of 37 *E. faecalis* proteins, including the heat-shock proteins DnaK and GroEL, and genes, including *ace*, *fsrB*, and *gelE* (Flahaut et al. 1997, Ran et al. 2013). In our work, expression of the heat-shock operon (OG1RF_11076-11080, *hrcA-dnaJ*), *ace* (OG1RF_10878), and *fsrB* (OG1RF_11528) was not significantly changed after growth in arginine, and expression of *gelE* (OG1RF_11526) was lower (Table S1). Finally, we compared our arginine RNAseq to a study that identified mutations in base-adapted *E. faecalis* OG1RF (Fitzgerald et al. 2023). We found little correlation between these mutations and the gene expression pattern in RNAseq. Multiple high pH-evolved clones had mutations in genes encoding the Opp peptide transport system, the Pst phosphate transport system, OG1RF_11160 (encoding a putative thioesterase), and CcpA (Fitzgerald et al. 2023). In our work, *oppABCDF* and OG1RF_11160 were upregulated, *ccpA* was downregulated, and there was no change in expression of the *pst* operon. Together, this suggests that some changes in gene expression after growth in arginine may be due to alkaline stress, but the majority of changes we measured using RNAseq did not correlate with known patterns of gene or protein expression in high pH. As such, these changes in gene expression may be specifically linked to arginine catabolism and not simply a change in culture pH.

Arginine affects antibiotic susceptibility and cell envelope permeability of *E. faecalis*

In *S. pyogenes*, the ADI pathway affects biofilm-associated antibiotic resistance (Freiberg et al. 2020). Therefore, we searched our RNAseq data to see whether any differentially expressed genes were linked to antibiotic resistance in *E. faecalis*. The *liaFSR* genes associated with daptomycin resistance (Arias et al. 2011, Reyes et al. 2015) were significantly downregulated after growth in arginine, but many genes involved in resistance to antibiotics that target the cell envelope, such as those encoding penicillin-binding proteins, were upregulated (Table 2). Expression of *croRS*, which mediates cephalosporin resistance (Comenge et al. 2003, Kellogg and Kristich 2016), was moderately upregulated, but expression of *ireK* was not significantly changed.

Based on this, we hypothesized that antibiotic susceptibility would be altered in arginine-grown *E. faecalis* relative to cells grown in untreated medium and tested this using disc diffusion assays (Fig. 4A). OG1RF was grown on agar plates supplemented with arginine or glucose in the presence of a panel of antibiotics (ampicillin, cephalothin, ceftriaxone, gentamicin, linezolid, penicillin, minocycline, and vancomycin). Relative to growth on glucose or untreated CBM, we observed smaller zones of clearance (indicating less susceptibility) for ampicillin and ceftriaxone, although only the difference in ampicillin was statistically significant (Fig. 4B). This is consistent with the increased expression of *croRS* in the RNAseq, as deletion of *croRS* in the strain JH2-2 led to greater susceptibility to ampicillin and ceftriaxone (Comenge et al. 2003). No arginine-dependent change in ampicillin susceptibility was observed with the *arcABCD* Tn mutants (Fig. S5A), suggesting the increased tolerance observed for OG1RF is due to arginine metabolism. We did not detect a change in OG1RF susceptibility to minocycline and linezolid, which target the ribosome. These results suggest that susceptibility to antibiotics targeting the cell envelope may be altered in arginine-rich environments such as the oral cavity or GTI.

Given the changes in gene expression and antibiotic susceptibility after growth in arginine, we next asked whether integrity of the cell envelope was impacted in arginine-grown cells. To test this, we carried out a cell envelope permeability assay in which the cell-impermeable LacZ substrate CPRG is added to cultures of cells constitutively expressing *lacZ* from a plasmid. Cleavage of CPRG, which produces a color change and can be measured by absorbance at 570 nm, can occur when the cell envelope is compromised (Paradis-Bleau et al. 2014, Djorić and Kristich 2015). We grew OG1RF constitutively expressing *lacZ* from plasmid pCJK205 (Djorić and Kristich 2015) in arginine, glycine, glucose, or untreated medium and quantified CPRG cleavage after 24 h growth (Fig. 4C). In 50 mM arginine, there was a

Table 2. Antibiotic resistance genes are differentially expressed in *E. faecalis* OG1RF after growth in arginine.

Locus tag (gene name)	Log2FC	Associated antibiotic
OG1RF_10417 (*pbp2A*)	3.91	β-Lactams, cephalosporins (Arbeloa et al. 2004, Kristich et al. 2014)
OG1RF_10724 (*pbpC*)	3.83	
OG1RF_10925 (*pbp1A*)	3.21	
OG1RF_11450 (*pbp1B*)	2.39	
OG1RF_11907 (*pbp4(5)*)	1.28	
OG1RF_12158 (*penA/pbpA(2B)*)	1.98	
OG1RF_12165	3.79	Streptomycin (Clark et al. 1999)
OG1RF_12193	1.33	Methicillin (Rigottier-Gois et al. 2011)
OG1RF_12211 (*liaR*)	−1.89	Daptomycin (Arias et al. 2011, Reyes et al. 2015)
OG1RF_12212 (*liaS*)	−1.47	
OG1RF_12213 (*liaF*)	−1.87	
OG1RF_12535 (*croR*)	1.54	Cephalosporins (Comenge et al. 2003)
OG1RF_12536 (*croS*)	1.48	

For genes where log2FC values are shown, $q < 0.05$.

significant increase in CPRG cleavage relative to the untreated control. There was no statistically significant change with cultures grown in glycine or glucose. No increase in CPRG cleavage was detected for the *arcD*:: Tn mutant carrying pCJK205 when grown in arginine (Fig. S5B). Together, these data demonstrate that growth in arginine changes antibiotic susceptibility and cell envelope permeability of *E. faecalis* and that these phenotypes are dependent on arginine metabolism.

Discussion

Arginine metabolism by *E. faecalis* affects polymicrobial interactions and promotes virulence of other pathogens (Keogh et al. 2016, Smith et al. 2022). Our work demonstrates that arginine also induces widespread changes in gene expression, biofilm formation, and antibiotic tolerance in *E. faecalis* (summarized in Fig. 5) and that some of these changes are species-specific based on what has been reported for other organisms. We propose that these effects on *E. faecalis* could happen in the context of polymicrobial environments and that this could impact stability and survival of these communities as a whole. Arginine concentrations vary across body sites in animals and humans. Plasma concentration in healthy adults is ∼100 µM (Zhang et al. 2016). In separate studies, arginine concentration ranged from 30 to 50 µM in the murine colon and small intestine (Hou et al. 2020, Menezes-Garcia et al. 2020), although this can increase with arginine-rich diets or supplementation (Grimble 2007, Hou et al. 2020). However, arginine levels can be higher in the oral cavity, as arginine-supplemented dentistry products contain between 1.5% and 8% (86–459 mM) arginine, and dietary intake can be tens of grams per day (Grimble 2007, Nascimento 2018). As such, it is of interest to determine how *E. faecalis* arginine metabolism affects microbial community composition and survival in multiple niches, as these dynamics may change based on local arginine concentration or arginine flux.

Similar to other Gram-positive bacteria, *E. faecalis* biofilm production decreased in the presence of arginine, which could have implications for how *E. faecalis* forms biofilms in arginine-rich environments. However, pre-formed *E. faecalis* biofilms were not disrupted by the same concentrations of arginine that reduced biofilm growth. High concentrations of arginine (250–500 mM) that were previously shown to destabilize *S. mutans* biofilms (Zheng et al. 2017) did not disrupt pre-grown *E. faecalis* biofilms in our work as measured by safranin staining. Previous work with *S. gordonii* also showed that treatment with exogenous arginine, but not glycine, weakened biofilms and led to increased removal by shear stress (Gloag et al. 2021). Although that work used higher concentrations (4% arginine and 0.23 M glycine) than our studies, we did not observe significant changes in aggregation or biofilm formation in the presence of glycine when used at the same concentration as arginine. Based on these differences in biofilm disruption across species, it is interesting to speculate that arginine could potentially promote selective removal or destabilization of non-*E. faecalis* bacteria in biofilms.

An additional outstanding question is the mechanism by which growth in arginine leads to changes in biofilm morphology. *Streptococcus mutans* biofilms grown with 1.5% arginine had reduced levels of exopolysaccharides and multi-cellular clusters or microcolonies (He et al. 2016). Conversely, we observed an increase in *E. faecalis* aggregation during planktonic and biofilm growth in arginine, although morphology changes are also evident in glucose-grown biofilms compared to untreated media. In our RNAseq, we found increased expression of genes in the Epa operon, which encodes for biosynthesis of the cell wall-associated enterococcal polysaccharide antigen (Teng et al. 2009, Guerardel et al. 2020). Epa modifications can alter *E. faecalis* biofilm morphology, leading to an increase in multi-cellular clusters or microcolonies instead of the flat monolayer biofilms typically formed *in vitro* by *E. faecalis* OG1RF (Dale et al. 2017, Korir et al. 2019). However, more work is needed to understand what specifically drives arginine-induced biofilm morphology rearrangement, how this varies in different bacterial species, and how that might translate to biofilm remodeling *in vivo*.

Growth in arginine also allowed us to observe effects on aggregates formed in liquid cultures separately from surface-associated biofilms. Distinct liquid aggregate and biofilm populations have been observed for *E. faecalis* and other bacteria grown in synovial fluid or serum (Sauer et al. 2022, Haeberle et al. 2024). Bacterial biofilms are often studied as surface-attached entities, but a revised model of biofilm development that incorporates aggregates in suspension has been proposed (Rumbaugh and Sauer 2020, Sauer et al. 2022). Such unattached aggregates are relevant in the environment and *in vivo*, and these clusters of cells are often recalcitrant to antibiotic killing like their surface-attached counterparts (Bjarnsholt et al. 2013, Sauer et al. 2022).

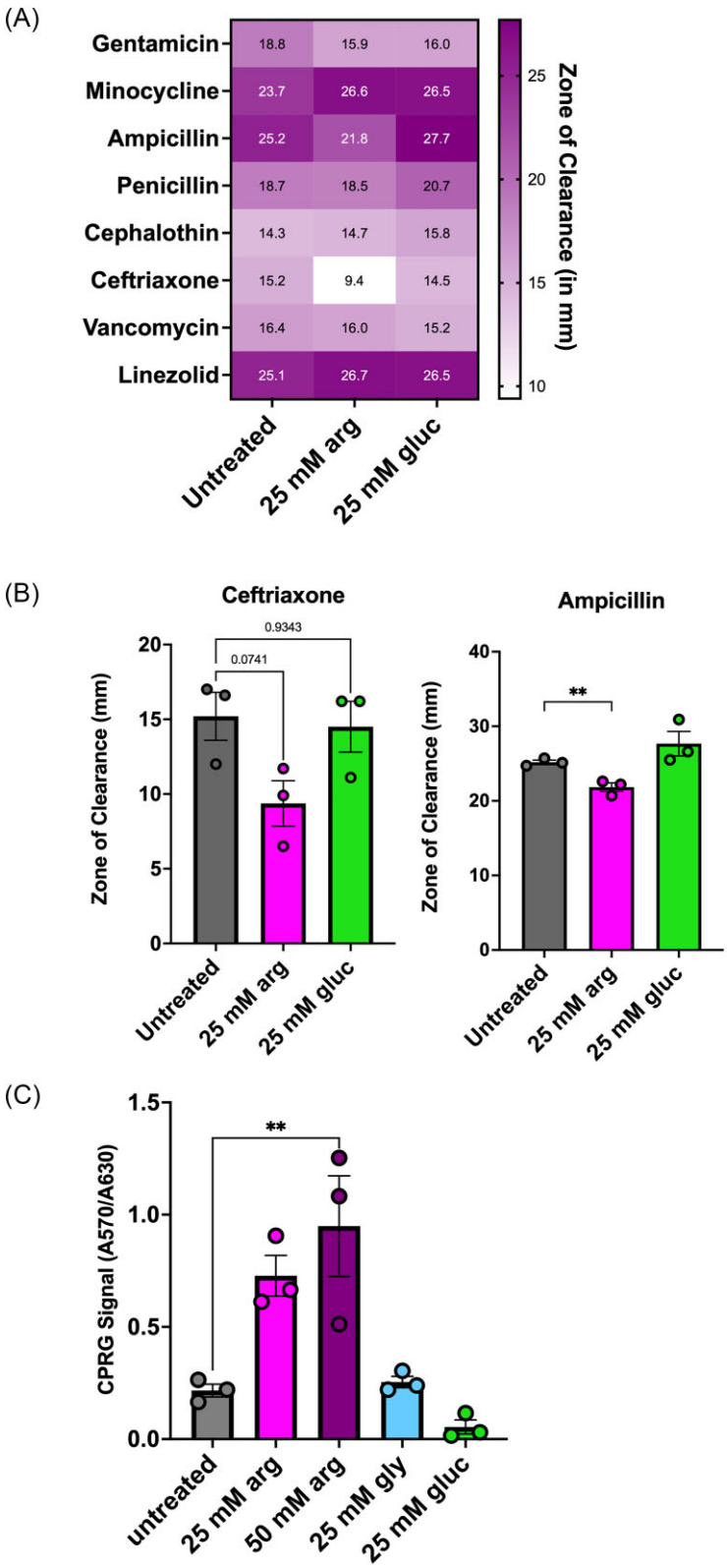

Figure 4. Growth with arginine affects cell envelope permeability and antibiotic resistance in *E. faecalis*. (A) Heatmap of zones of inhibition (measured in mm) of antibiotic disc diffusion assay. Cells were grown on CBM agar plates supplemented with arginine or glucose (25 mM). Discs measured 9 mm in diameter. Data represent the average of three independent biological replicates. (B) Individual values of disc diffusion zones for ceftriaxone and ampicillin. (C) Measurement of signal from cleavage of CPRG (A570) relative to growth (A630). For panels (B) and (C), each data point represents an independent biological replicate. Statistical significance was determined using one-way ANOVA with Dunnett's test for multiple comparisons. $^{**}P < .01$.

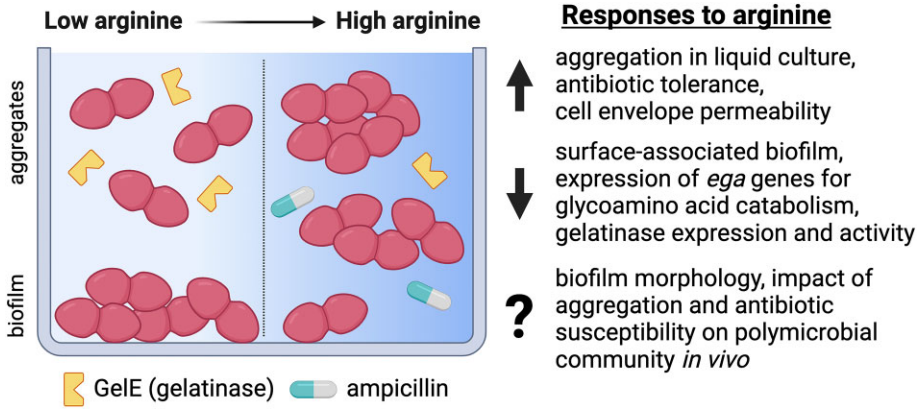

Figure 5. Model summarizing the response of *E. faecalis* to arginine. In the absence of arginine (or the presence of low arginine), *E. faecalis* forms robust surface-attached biofilms and does not form aggregates in liquid culture. Upon exposure to high concentrations of arginine (25 or 50 mM), global gene expression and phenotype changes occur. This leads to increased aggregation of liquid cultures, increased tolerance to antibiotics, such as ampicillin, and increased cell envelope permeability with a concomitant reduction in surface-associated biofilm formation and production of gelatinase. It is yet unknown what drives biofilm remodeling or how these gene expression and phenotypic changes impact survival within a polymicrobial infection, such as those where cross-feeding mediated by *E. faecalis* arginine metabolism promotes biofilm formation and virulence of other pathogens (Keogh et al. 2016, Smith et al. 2022).

Aggregates may promote survival or lead to decreased fitness depending on the environment in which they form. Some bacteria form unattached aggregates in wounds and the joint cavity (Sauer et al. 2022), but these same clusters may be removed from the host more than attached biofilms in sites with high fluid flow or turnover. Therefore, *E. faecalis* aggregation may differentially impact fitness depending on the niche in which these aggregates form. We do not think the liquid-grown aggregates of *E. faecalis* we observed came from shearing of attached biofilm cells, given that *E. faecalis* OG1RF does not form robust biofilms on the glass tubes used in these experiments. Based on the gene expression changes detected using RNAseq, we speculate that liquid aggregates formed during growth in arginine could be driven by increased surface polysaccharide synthesis or by overproduction of surface adhesins. However, this needs to be rigorously tested.

We also observed differences in gene expression of arginine-grown *E. faecalis* compared to other oral bacteria. In *S. mutans*, expression of the *dnaK* stress response operon was upregulated after growth in 1.5% arginine (Chakraborty and Burne 2017). However, in our RNAseq, expression of the *dnaJK* stress response genes was not significantly changed during growth in arginine. This could potentially be relevant for oral health as arginine is used in dentistry to control plaque and prevent caries (cavities) (Nascimento 2018). *E. faecalis* is not considered part of the normal oral microbiome but is a leading cause of infected root canals (Wang et al. 2012, Pinto et al. 2023), so it is interesting to consider whether the relative abundance of *E. faecalis* in the oral cavity would be affected by arginine treatment in healthy patients or those with active root canal infections. Given that we measured a decrease in antibiotic susceptibility of *E. faecalis* during growth in arginine, it is also interesting to consider how the use of arginine in the oral cavity could affect virulence of *E. faecalis*. We observed arginine-related *E. faecalis* phenotypes at relatively low concentrations (25 and 50 mM) compared to other studies examining the impact of arginine treatment on the oral microbiome, co-culture biofilm structure and composition, exopolysaccharide, and gene expression (He et al. 2016, Zheng et al. 2017). Therefore, it is possible that *E. faecalis* may respond to arginine at sub-clinical levels relative to what is used in dentistry applications. However, the broader impact of how this affects *E. faecalis* biofilms and antibiotic resistance in the oral cavity or other body sites is yet undetermined.

Arginine metabolism can confer benefits to bacteria during adaptation to a mammalian niche. We found some overlap in arginine-induced gene expression changes and other studies on *E. faecalis* growth in alkaline stress (Flahaut et al. 1997, Ran et al. 2013, 2015), and previous work showed that alkaline-adapted *E. faecalis* acquired cross-resistance to bile salts (Flahaut et al. 1997). Therefore, arginine exposure in the oral cavity or GI tract (and the resulting changes in pH and gene expression) could prime *E. faecalis* for survival against bile salts and other stressors. ADI pathway-derived ammonia was hypothesized to promote survival of *Staphylococcus epidermidis* during biofilm growth, as expression of the ADI pathway was upregulated in biofilms (Lindgren et al. 2014). Additionally, arginine metabolism through an ADI pathway encoded on a mobile element in *S. aureus* USA300 was important for survival in skin-mimicking acidic conditions (Thurlow et al. 2013). ADI pathways were identified in mammalian-associated Saccharibacteria but not those isolated from environmental habitats, and the presence of arginine maintained infectivity of *Nanosynbacter lyticus* strain TM7x in conditions that mimicked the oral cavity (Tian et al. 2022). However, the presence of arginine promoted cell membrane integrity in TM7x, whereas we demonstrated here that growth in arginine disrupts cell envelope integrity in *E. faecalis*. Together, this suggests that while the ADI pathway may promote survival of diverse bacteria *in vivo*, the mechanisms by which this occurs can differ across species.

The ADI pathway has previously been linked to antibiotic tolerance during oxidative stress and biofilm growth in *E. faecalis* and other bacteria. Upregulation of the ADI operon was associated with restored vancomycin tolerance in *E. faecalis* mutants lacking *sodA* (encoding superoxide dismutase), and disruption of the ADI pathway in a *sodA* mutant background led to increased killing by vancomycin relative to the *sodA* mutant alone (Ladjouzi et al. 2015). In *S. pyogenes*, the ADI pathway is important for biofilm-associated antibiotic resistance *in vitro* and in an *in vivo* animal model (Freiberg et al. 2020). Here, we found changes in the expression of multiple genes linked to *E. faecalis* antibiotic tolerance and found that *E. faecalis* grown with arginine was less susceptible than control cells to ampicillin and ceftriaxone. Based on this,

it is interesting to speculate that arginine metabolism in various body sites may contribute to tolerance of *E. faecalis* to antibiotics and that this could contribute to persistence or overgrowth during antibiotic treatment. Additionally, it is unknown how arginine metabolism by *E. faecalis* might influence antibiotic susceptibility within a complex environment like a polymicrobial community. Altered susceptibility could make *E. faecalis* clearance more difficult in niches where arginine levels are elevated. This potentially could contribute to *E. faecalis* overgrowth if some bacteria in a polymicrobial environment are cleared by ampicillin or ceftriaxone, but *E. faecalis* has increased tolerance due to arginine metabolism. Because the arginine-dependent effect on tolerance was not observed for all antibiotics, this is likely to be compound-specific in practice. However, deeper insight into how *E. faecalis* antibiotic susceptibility is affected by nutrients, whether this happens in a niche-specific manner, and how this in turn affects survival and clearance of polymicrobial infections could potentially be leveraged to guide treatment choices or create novel therapeutic practices.

Our work shows that *E. faecalis* growth and biofilm formation are altered in the presence of arginine. Importantly, we also identified species-specific differences in expression of stress response genes, biofilm destabilization, and biofilm architecture relative to what was previously known about arginine-induced changes in Gram-positive bacteria. Together, this work provides a better understanding of how *E. faecalis* responds to growth in arginine independent of cross-feeding that promotes virulence of other pathogens and provides a platform from which the impact of *E. faecalis* gene expression changes on polymicrobial interactions and infections can be studied in addition to phenotypes mediated by arginine metabolism through the ADI pathway.

Acknowledgments

We thank the Dunny and Willett labs for helpful input on the manuscript. The content is solely the responsibility of the authors and does not necessarily represent the official views of the National Institutes of Health. This work was also supported by the resources and staff at the University of Minnesota Genomics Center (RRID: SCR_012413).

Supplementary data

Supplementary data is available at FEMSMC *Journal* online.

Conflict of interest: None declared.

Funding

This work was supported by National Institutes of Health grants R01AI122742 to G.M.D. and R00AI151080 to J.L.E.W. plus start-up funds from the University of Minnesota to J.L.E.W.

Data availability

Raw sequencing files and processed data have been deposited in the NCBI GEO database with accession number GSE268264.

References

Abranches J, Tijerina P, Avilés-Reyes A *et al.* The cell wall-targeting antibiotic stimulon of *Enterococcus faecalis*. *PLoS One* 2014;**8**:e64875.

Afonina I, Tien B, Nair Z *et al.* The composition and function of *Enterococcus faecalis* membrane vesicles. *Microlife* 2021;**2**:uqab002.

Andrews S. FastQC: a quality control tool for high throughput sequence data. 2010. https://www.bioinformatics.babraham.ac.uk/projects/fastqc/ (16 January 2020, date last accessed).

Arbeloa A, Segal H, Hugonnet J-E *et al.* Role of class A penicillin-binding proteins in PBP5-mediated beta-lactam resistance in *Enterococcus faecalis*. *J Bacteriol* 2004;**186**:1221–8.

Arias CA, Panesso D, Mcgrath DM *et al.* Genetic basis for *in vivo* daptomycin resistance in enterococci. *N Engl J Med* 2011;**365**:892–900.

Barcelona-Andrés Belén, Marina A, Rubio V. Gene structure, organization, expression, and potential regulatory mechanisms of arginine catabolism in *Enterococcus faecalis*. *J Bacteriol* 2002;**184**:6289–300.

Béliveau C, Potvin C, Trudel J *et al.* Cloning, sequencing, and expression in *Escherichia coli* of a *Streptococcus faecalis* autolysin. *J Bacteriol* 1991;**173**:5619–23.

Bjarnsholt T, Alhede M, Alhede M *et al.* The *in vivo* biofilm. *Trends Microbiol* 2013;**21**:466–74.

Bolger AM, Lohse M, Usadel B. Trimmomatic: a flexible trimmer for Illumina sequence data. *Bioinformatics* 2014;**30**:2114–20.

Buist G, Steen A, Kok J *et al.* LysM, a widely distributed protein motif for binding to (peptido)glycans. *Mol Microbiol* 2008;**68**:838–47.

Burne RA, Marquis RE. Alkali production by oral bacteria and protection against dental caries. *FEMS Microbiol Lett* 2000;**193**:1–6.

Chakraborty B, Burne RA. Effects of arginine on *Streptococcus mutans* growth, virulence gene expression, and stress tolerance. *Appl Environ Microb* 2017;**83**:e00496–17.

Ch'ng J-H, Muthu M, Chong KKL *et al.* Heme cross-feeding can augment *Staphylococcus aureus* and *Enterococcus faecalis* dual species biofilms. *ISME J* 2022;**16**:2015–26.

Clark NC, Olsvik Ø, Swenson JM *et al.* Detection of a streptomycin/spectinomycin adenylyltransferase gene (aadA) in *Enterococcus faecalis*. *Antimicrob Agents Chemother* 1999;**43**:157–60.

Combret V, Rincé I, Budin-Verneuil A *et al.* Utilization of glycoprotein-derived N-acetylglucosamine-L-asparagine during *Enterococcus faecalis* infection depends on catabolic and transport enzymes of the glycosylasparaginase locus. *Res Microbiol* 2023;**175**:104169.

Comenge Y, Quintiliani R, Li L *et al.* The CroRS two-component regulatory system is required for intrinsic beta-lactam resistance in *Enterococcus faecalis*. *J Bacteriol* 2003;**185**:7184–92.

Dale JL, Nilson JL, Barnes AMT *et al.* Restructuring of *Enterococcus faecalis* biofilm architecture in response to antibiotic-induced stress. *NPJ Biofilms Microbiomes* 2017;**3**:15.

Darnell RL, Knottenbelt MK, Todd Rose FO *et al.* Genomewide profiling of the *Enterococcus faecalis* transcriptional response to teixobactin reveals CroRS as an essential regulator of antimicrobial tolerance. *mSphere* 2019;**4**:e00228–19.

Deibel RH. Utilization of arginine as an energy source for the growth of *Streptococcus faecalis*. *J Bacteriol* 1964;**87**:988–92.

Djorić D, Kristich CJ. Oxidative stress enhances cephalosporin resistance of *Enterococcus faecalis* through activation of a two-component signaling system. *Antimicrob Agents Chemother* 2015;**59**:159–69.

Dunny G, Funk C, Adsit J. Direct stimulation of the transfer of antibiotic resistance by sex pheromones in *Streptococcus faecalis*. *Plasmid* 1981;**6**:270–8.

Eckert C, Lecerf M, Dubost L *et al.* Functional analysis of AtlA, the major N-acetylglucosaminidase of *Enterococcus faecalis*. *J Bacteriol* 2006;**188**:8513–9.

Fitzgerald BA, Wadud A, Slimak Z *et al.*. *Enterococcus faecalis* OG1RF evolution at low pH selects fusidate-sensitive mutants in elonga-

tion factor G and at high pH selects defects in phosphate transport. *Appl Environ Microb* 2023;**89**:e0046623.
Flahaut S, Hartke A, Giard JC *et al.* Alkaline stress response in *Enterococcus faecalis*: adaptation, cross-protection, and changes in protein synthesis. *Appl Environ Microb* 1997;**63**:812–4.
Freiberg JA, Le Breton Y, Harro JM *et al.* The arginine deiminase pathway impacts antibiotic tolerance during biofilm-mediated *Streptococcus pyogenes* infections. *mBio* 2020;**11**:e00919–20.
Gaca AO, Lemos JA. Adaptation to adversity: the intermingling of stress tolerance and pathogenesis in enterococci. *Microbiol Mol Biol Rev* 2019;**83**:e00008–19.
García-Solache M, Rice LB. The *Enterococcus*: a model of adaptability to its environment. *Clin Microbiol Rev* 2019;**32**:e00058–18.
Gaston JR, Andersen MJ, Johnson AO *et al. Enterococcus faecalis* polymicrobial interactions facilitate biofilm formation, antibiotic recalcitrance, and persistent colonization of the catheterized urinary tract. *Pathogens* 2020;**9**:835.
Gaston JR, Johnson AO, Bair KL *et al.* Polymicrobial interactions in the urinary tract: is the enemy of my enemy my friend? *Infect Immun* 2021;**89**:1–29.
Gilmore MS, Lebreton F, Van Schaik W. Genomic transition of enterococci from gut commensals to leading causes of multidrug-resistant hospital infection in the antibiotic era. *Curr Opin Microbiol* 2013;**16**:10–6.
Gilmore MS, Salamzade R, Selleck E *et al.* Genes contributing to the unique biology and intrinsic antibiotic resistance of *Enterococcus faecalis*. *mBio* 2020;**11**:e02962–20.
Gloag ES, Wozniak DJ, Wolf KL *et al.* Arginine induced *Streptococcus gordonii* biofilm detachment using a novel rotating-disc rheometry method. *Front Cell Infect Microbiol* 2021;**11**:784388.
Goh HMS, Yong MHA, Chong KKL *et al.* Model systems for the study of enterococcal colonization and infection. *Virulence* 2017;**8**:1525–62.
Grimble GK. Adverse gastrointestinal effects of arginine and related amino acids. *J Nutr* 2007;**137**:1693S–701S.
Guerardel Y, Sadovskaya I, Maes E *et al.* Complete structure of the enterococcal polysaccharide antigen (EPA) of vancomycin-resistant *Enterococcus faecalis* V583 reveals that EPA decorations are teichoic acids covalently linked to a rhamnopolysaccharide backbone. *mBio* 2020;**11**:e00277–20.
Haeberle AL, Greenwood-Quaintance KE, Zar S *et al.* Genotypic and phenotypic characterization of *Enterococcus faecalis* isolates from periprosthetic joint infections. *Microbiol Spectr* 2024;**12**:e0056524.
He J, Hwang G, Liu Y *et al.* l-arginine modifies the exopolysaccharide matrix and thwarts *Streptococcus mutans* outgrowth within mixed-species oral biofilms. *J Bacteriol* 2016;**198**:2651–61.
Hirose Y, Yamaguchi M, Sumitomo T *et al. Streptococcus pyogenes* upregulates arginine catabolism to exert its pathogenesis on the skin surface. *Cell Rep* 2021;**34**:108924.
Hou Q, Dong Y, Huang J *et al.* Exogenous L-arginine increases intestinal stem cell function through CD90+ stromal cells producing mTORC1-induced Wnt2b. *Commun Biol* 2020;**3**:611.
Jakubovics NS, Robinson JC, Samarian DS *et al.* Critical roles of arginine in growth and biofilm development by *Streptococcus gordonii*. *Mol Microbiol* 2015;**97**:281–300.
Kellogg SL, Kristich CJ. Functional dissection of the CroRS two-component system required for resistance to cell wall stressors in *Enterococcus faecalis*. *J Bacteriol* 2016;**198**:1326–36.
Keogh D, Tay WH, Ho YY *et al.* Enterococcal metabolite cues facilitate interspecies niche modulation and polymicrobial infection. *Cell Host Microbe* 2016;**20**:493–503.
Kolderman E, Bettampadi D, Samarian D *et al.* L-arginine destabilizes oral multi-species biofilm communities developed in human saliva. *PLoS One* 2015;**10**:e0121835.
Korir ML, Dale JL, Dunny GM. Role of *epaQ*, a previously uncharacterized *Enterococcus faecalis* gene, in biofilm development and antimicrobial resistance. *J Bacteriol* 2019;**201**:e00078–19.
Kristich CJ, Rice LB, Arias CA. Enterococcal infection—treatment and antibiotic resistance. In Editor-in-chief Gilmore MS, Clewell DB, Ike Y *et al.* (eds), *Enterococci: From Commensals to Leading Causes of Drug Resistant Infection*. Boston: Massachusetts Eye and Ear Infirmary, 2014.
Ladjouzi R, Bizzini A, Van Schaik W *et al.* Loss of antibiotic tolerance in SoD-deficient mutants is dependent on the energy source and arginine catabolism in enterococci. *J Bacteriol* 2015;**197**:3283–93.
Lebreton F, Manson AL, Saavedra JT *et al.* Tracing the enterococci from paleozoic origins to the hospital. *Cell* 2017;**169**:849–61.
Leuck A-M, Johnson JR, Dunny GM. A widely used *in vitro* biofilm assay has questionable clinical significance for enterococcal endocarditis. *PLoS One* 2014;**9**:e107282.
Lindgren JK, Thomas VC, Olson ME *et al.* Arginine deiminase in *Staphylococcus epidermidis* functions to augment biofilm maturation through pH homeostasis. *J Bacteriol* 2014;**196**:2277–89.
McBride SM, Fischetti VA, Leblanc DJ *et al.* Genetic diversity among *Enterococcus faecalis*. *PLoS One* 2007;**2**:e582.
McClure R, Balasubramanian D, Sun Y *et al.* Computational analysis of bacterial RNA-seq data. *Nucleic Acids Res* 2013;**41**:e140.
Manias DA, Dunny GM. Expression of adhesive pili and the collagen-binding adhesin ace is activated by ArgR family transcription factors in *Enterococcus faecalis*. *J Bacteriol* 2018;**200**:e00269–18.
Manna AC, Leo S, Girel S *et al.* Teg58, a small regulatory RNA, is involved in regulating arginine biosynthesis and biofilm formation in *Staphylococcus aureus*. *Sci Rep* 2022;**12**:14963.
Menezes-Garcia Z, Kumar A, Zhu W *et al.* l-arginine sensing regulates virulence gene expression and disease progression in enteric pathogens. *Proc Natl Acad Sci USA* 2020;**117**:12387–93.
Muller C, Massier S, Le Breton Y *et al.* The role of the CroR response regulator in resistance of *Enterococcus faecalis* to D-cycloserine is defined using an inducible receiver domain. *Mol Microbiol* 2018;**107**:416–27.
Nascimento MM. Potential uses of arginine in dentistry. *Adv Dent Res* 2018;**29**:98–103.
Nascimento MM, Browngardt C, Xiaohui X *et al.* The effect of arginine on oral biofilm communities. *Mol Oral Microbiol* 2014;**29**:45–54.
Opsata M, Nes IF, Holo H. Class IIa bacteriocin resistance in *Enterococcus faecalis* V583: the mannose PTS operon mediates global transcriptional responses. *BMC Microbiol* 2010;**10**:224.
Paradis-Bleau C, Kritikos G, Orlova K *et al.* A genome-wide screen for bacterial envelope biogenesis mutants identifies a novel factor involved in cell wall precursor metabolism. *PLoS Genet* 2014;**10**:e1004056.
Pinto KP, Barbosa AFA, Silva EJNL *et al.* What is the microbial profile in persistent endodontic infections? A scoping review. *J Endod* 2023;**49**:786–98.
Ran S, He Z, Liang J. Survival of *Enterococcus faecalis* during alkaline stress: changes in morphology, ultrastructure, physiochemical properties of the cell wall and specific gene transcripts. *Arch Oral Biol* 2013;**58**:1667–76.
Ran S, Liu B, Jiang W *et al.* Transcriptome analysis of *Enterococcus faecalis* in response to alkaline stress. *Front Microbiol* 2015;**6**:795.
Reyes J, Panesso D, Tran TT *et al.* A liaR deletion restores susceptibility to daptomycin and antimicrobial peptides in multidrug-resistant *Enterococcus faecalis*. *J Infect Dis* 2015;**211**:1317–25.
Rigottier-Gois L, Alberti A, Houel A *et al.* Large-scale screening of a targeted *Enterococcus faecalis* mutant library identifies envelope fitness factors. *PLoS One* 2011;**6**:e29023.

Rumbaugh KP, Sauer K. Biofilm dispersion. *Nat Rev Micro* 2020;**18**:571–86.
Sauer K, Stoodley P, Goeres DM *et al.* The biofilm life cycle: expanding the conceptual model of biofilm formation. *Nat Rev Micro* 2022;**20**:608–20.
Schindelin J, Arganda-Carreras I, Frise E *et al.* Fiji: an open-source platform for biological-image analysis. *Nat Methods* 2012;**9**:676–82.
Smith AB, Jenior ML, Keenan O *et al.* Enterococci enhance *Clostridioides difficile* pathogenesis. *Nature* 2022;**611**:780–86.
Tan CAZ, Antypas H, Kline KA. Overcoming the challenge of establishing biofilms *in vivo*: a roadmap for enterococci. *Curr Opin Microbiol* 2020;**53**:9–18.
Tan CAZ, Lam LN, Biukovic G *et al. Enterococcus faecalis* antagonizes *Pseudomonas aeruginosa* growth in mixed-species interactions. *J Bacteriol* 2022;**204**:e0061521.
Teng F, Singh KV, Bourgogne A *et al.* Further characterization of the epa gene cluster and Epa polysaccharides of *Enterococcus faecalis*. *Infect Immun* 2009;**77**:3759–67.
Thurlow LR, Joshi GS, Clark JR *et al.* Functional modularity of the arginine catabolic mobile element contributes to the success of USA300 methicillin-resistant *Staphylococcus aureus*. *Cell Host Microbe* 2013;**13**:100–7.
Tian J, Utter DR, Cen L *et al.* Acquisition of the arginine deiminase system benefits epiparasitic Saccharibacteria and their host bacteria in a mammalian niche environment. *Proc Natl Acad Sci USA* 2022;**119**: e2114909119.
Tien BYQ, Goh HMS, Chong KKL *et al. Enterococcus faecalis* promotes innate immune suppression and polymicrobial catheter-associated urinary tract infection. *Infect Immun* 2017;**85**: e00378–17.
Tjaden B. De novo assembly of bacterial transcriptomes from RNA-seq data. *Genome Biol* 2015;**16**:1.
Wang Q-Q, Zhang C-F, Chu C-H *et al.* Prevalence of *Enterococcus faecalis* in saliva and filled root canals of teeth associated with apical periodontitis. *Int J Oral Sci* 2012;**4**:19–23.
Wagner M, Sonntag D, Grimm R *et al.* Substrate-specific selenoprotein B of glycine reductase from *Eubacterium acidaminophilum*. Biochemical and molecular analysis. *Eur J Biochem* 1999;**260**: 38–49.
Willett JLE, Dale JL, Kwiatkowski LM *et al.* Comparative biofilm assays using *Enterococcus faecalis* OG1RF identify new determinants of biofilm formation. *mBio* 2021;**12**:e0101121.
Willett JLE, Ji M, Dunny GM. Exploiting biofilm phenotypes for functional characterization of hypothetical genes in *Enterococcus faecalis*. *NPJ Biofilms Microbiomes* 2019;**5**:23.
Zhang W, Sun G, Likhodii S *et al.* Metabolomic analysis of human plasma reveals that arginine is depleted in knee osteoarthritis patients. *Osteoarthritis Cartilage* 2016;**24**:827–34.
Zhang Y, Turanov AA, Hatfield DL *et al.* In silico identification of genes involved in selenium metabolism: evidence for a third selenium utilization trait. *BMC Genomics* 2008;**9**:251.
Zheng X, He J, Wang L *et al.* Ecological effect of arginine on oral microbiota. *Sci Rep* 2017;**7**:7206.

Received 27 May 2024; **revised** 26 August 2024; **accepted** 24 September 2024